Lab on a Chip

Development of a self-powered digital LAMP microfluidic chip (SP-dChip) for the detection of emerging viruses

Journal:	*Lab on a Chip*
Manuscript ID	LC-ART-03-2024-000265.R1
Article Type:	Paper
Date Submitted by the Author:	21-May-2024

Complete List of Authors:	Kasputis, Tom; Virginia Polytechnic Institute and State University, Biological Systems Engineering Yeh, Po-Chen; University of California Berkeley Liu, Li; University of California Riverside, Marano, Jeffery; Virginia Polytechnic Institute and State University Weger-Lucarelli, James; Virginia Tech, Biomedical Sciences and Pathobiology Du, Ke; University of California Riverside, ; RIT, Lin, Liwei; University of California Berkeley Chen, Juhong; University of California Riverside, Bioengineering; Virginia Polytechnic Institute and State University, Biological Systems Engineering

ARTICLE

Development of a self-powered digital LAMP microfluidic chip (SP-dChip) for the detection of emerging viruses

Tom Kasputis, [a] Po-Chen Yeh, [b] Li Liu, [c] Jeffrey Marano, [d,e] James Weger-Lucarelli, [d] Ke Du, [c] Liwei Lin, [*b] and Juhong Chen [*a,f]

.Received 00th January 20xx,
Accepted 00th January 20xx

DOI: 10.1039/x0xx00000x

Point-of-care (POC) diagnostics have emerged as a crucial technology for emerging pathogen detections to enable rapid and on-site detection of infectious diseases. However, current POC devices often suffer from limited sensitivity with poor reliability to provide quantitative readouts. In this paper, we present a self-powered digital loop-mediated isothermal amplification (dLAMP) microfluidic chip (SP-dChip) for the rapid and quantitative detection of nucleic acids. The SP-dChip utilizes a vacuum lung design to passively digitize samples into individual nanoliter wells for high-throughput analysis. The superior digitization scheme is further combined with reverse transcription loop-mediated isothermal amplification (RT-LAMP) to demonstrate dLAMP detection of Zika Virus (ZIKV). Firstly, the LAMP assay is loaded into the chip and passively digitized into individual wells. Mineral oil is then pipetted through the chip to differentiate each well as an individual reactor. The chip did not require any external pumping or power input for rapid and reliable results to detect ZIKA RNA as low as 100 copies/µL within one hour. As such, this SP-dChip offers a new class of solutions for truly affordable, portable, and quantitative POC detections for emerging viruses.

Introduction

Point-of-care (POC) diagnostics have become an imperative technology for emerging pathogen detections. The ability to reliably detect infectious diseases on-site is vital for public health across the globe. POC diagnostics has surged in popularity due to its unrivaled timeliness and accessibility when compared to laboratory diagnostics. By increasing POC-based detections, the spread of disease and hospital visits can be reduced to lower both sickness and death rates.[1] However, current POC devices are far from ideal due to the lack of sensitivity and reliability, which hinder the impact of on-site diagnostics for the detection of emerging pathogens.

A desirable POC diagnostics system is rapid, affordable, reliable, and user-friendly.[2] Numerous innovative technologies have been developed for on-site pathogen detections, including enzyme-linked immunoassay (ELISA)[3, 4], surface-enhanced Raman spectroscopy (SERS)[5, 6], surface plasmon resonance (SPR)[7], and electrochemical biosensors[8]. These technologies often rely on expensive and extensive pre-processing methods.[9] Additionally, most POC sensors only provide positive/negative readouts instead of quantitative reuslts.[10] This limits the information on specificity and sensitivity, leading to potential false positives and false negatives from bulk solutions. Sample digitization provides a pragmatic solution for on-site quantitative POC sensing.[11, 12] For example, digital nucleic acid amplification has been shown to reduce the risk of primer dimerization while also increasing sensitivity using nanoliter digitization volumes.[13] Previously, various methods have been developed to digitize sample solutions, such as electrowetting[14], differential wetting[15], and droplet digitization[16]. However, these methods are rather complex and difficult to reproduce on a large scale. Thus, there is a need to develop simple yet robust quantitative sensors for POC diagnostics.

The most promising technology for sample digitization is microfluidics.[12, 17]. In the past decades, microfluidic technologies have revolutionized molecular diagnostics by reducing the necessary size for complex analytical systems.[18-20] Due to their simplicity, portability, and affordability, microfluidic devices can serve as an excellent platform for POC diagnostics,[21] such as compartmentalizing a single DNA/RNA copy into a small volume for digitization.[22] The ability to manipulate a nano-liter well or droplet as an independent reactor allows microfluidic devices to provide a high-throughput platform for analysis.[23] Compared to bulk systems, nano-liter reactors have shown a 1000-fold increase in throughput and a 50% reduction in detection time by generating a high-density environment and concentrating the diffusible signals.[24, 25] Furthermore, enclosing the entire analysis within these nano-liter wells can reduce potential

[a.] Department of Biological Systems Engineering, Virginia Tech, Blacksburg, VA, USA.
[b.] Department of Mechanical Engineering, University of California, Berkeley, CA, USA.
[c.] Department of Chemical and Environmental Engineering, University of California, Riverside, CA, USA.
[d.] Department of Biomedical Sciences and Pathobiology, Virginia Tech, Blacksburg, VA, USA.
[e.] Department of Biomedical Science, Colorado State, Fort Collins, CO, USA.
[f.] Department of Bioengineering, University of California, Riverside, CA, USA. E-mail: jchen@ucr.edu

contamination, consume fewer reagents, and enhance sensitivity, specificity, and reliability.[26]

While microfluidic systems provide many advantages for POC diagnostics and digitization, they often require complex control units and high-power consumption external pumping systems. For example, pressure controllers, centrifugal tools, and syringe pumps are all commonly used to control liquid flow in microfluidic systems,[27] and the external pumps further limit their portability and practical applications.[28] Hand-powered systems have been developed to address this issue,[29, 30] however, these systems require manual user inputs, which is challenging for non-trained personnel to replicate reliable results. Passive microfluidic systems can offer a user-friendly diagnostic experience without using any external power by means of osmotic, capillary-driven, or pressure-driven techniques.[31] However, current passively driven microfluidic devices are sensitive to clogging or backflow issues.[31-33] Thus, there is a vast need for the development of the next generation of passive microfluidic devices for sample digitization and quantitative detection.

Herein, we have demonstrated a self-powered digital loop-mediate isothermal amplification (dLAMP) microfluidic chip (SP-dChip) for the nano-liter reverse-transcription LAMP (RT-LAMP) process, providing a path for rapid and quantitative detection of genetic pathogens. This SP-dChip utilizes a vacuum lung system to digitize samples into each nanoliter well as individual reactors for quantitative test values. The chip is first vacuum sealed to reduce air pressure in the cavities, allowing for the passive fluidic flow through the channel once the vacuum bag is opened. Within the chip, reverse transcription and LAMP reactions are performed in each individual well for rapid on-site nucleic acid quantification. As a proof-of-concept, the SP-dChip has demonstrated the quantitative detection of Zika Virus (ZIKV) with a detection limit of 100 ZIKV RNA copies/µL within one hour. When compared with the current standards for POC detection, our system exhibits superior user-friendliness, portability, and robustness. As such, this microfluidic device could improve POC diagnostics in many areas to assist public health through improved detection of emerging viruses.

Materials and Methods

Materials and chemicals

All LAMP primers were purchased from Integrated DNA Technologies (Coralville, IA). The ZIKV RNA was isolated and provided by Dr. James Weger-Lucarelli in the Department of Biomedical Sciences and Pathobiology at Virginia Tech. The Benzonase and RNAse A used for RNA extraction were purchased from Millipore Sigma (Burlington, MA). WarmStart Fluorescent LAMP kit was purchased from New England Biolabs (Ipswich, MA). Fluorinert FC-40 mineral oil was purchased from Sigma-Aldrich (Burlington, MA). The Sylgard 184 silicone elastomer kit was purchased from the Dow Corning Corporation (Midland, MI). The microscope slides (1" x 3") were purchased from Amscope, and the vacuum-sealable bags (8" x 12") were purchased from Weston Brands (Southern Pines, NC).

Instrumentation

A 5CFM DC-142N vacuum pump (JB Industries, Aurora, IL) was used for PDMS degassing. For oxygen plasma bonding, a corona treater (BD-20AC Electro-Technic Products, Chicago, IL) was used. The chips were vacuum sealed using a professional advantage vacuum sealer (Weston Brands, Southern Pines, NC). A Mini-Incubator (VWR, Radnor, PA) was used for chip manufacturing and dLAMP amplification. Fluorescent analysis was performed using a Real-Time PCR machine (QuantStudio 3, Thermo Fisher Scientific, Waltham, MA). Gel electrophoresis was performed using a horizontal electrophoresis system (Thermo Fisher Scientific, Waltham, MA) and agarose gels, and fluorescent samples were imaged using an iBright 1500 Imager (Invitrogen, Thermo Fisher Scientific, Waltham, MA).

Fabrication of the microfluidic chip

The microfluidic pattern was designed using AutoCAD software (Autodesk, San Rafael, CA) and fabricated on a silicon wafer following standard photolithography.[28] Briefly, the silicon wafer was spin-coated with SU-8 photoresist and exposed to UV light with protection from a photomask. The UV exposure led to the crosslinking of SU-8 photoresist under the transparent area of the photomask, resulting in the formation of microfluidic patterns. The height of the pattern was confirmed to be around 88 µm using a profilometer.

The microfluidic chips were constructed using standard soft lithography (**Fig. S1**).[28] A mixture of Sylgard 184 (30 g, a 10:1 ratio of base to curing agent) was mixed and then poured onto a reusable mold on the photoresist. The PDMS mixture was then degassed using a vacuum pump for 20 min and then incubated at 65°C for at least two hours, forming a PDMS slab of six chips around 3.5 mm thick. The chips were then cut from the mold and protected with parafilm. Holes (0.5 mm in diameter) were then punched in the designated inlets and outlets for the channel and covered with aluminum foil. Afterward, the PDMS chips were bonded to clear glass microscope slides via oxygen plasma bonding using a corona treater. This treatment introduces polar functional groups on the PDMS, changing the surface properties from hydrophobic to hydrophilic for the bonding process. The bonded chips were then incubated at 65°C for at least two hours with light pressure to improve the binding of the PDMS to the glass slide. Once adhered to the glass slide, the chips were placed in a vacuum-sealable bag and sealed using a vacuum sealer. The chips were left at room temperature overnight to create the vacuum pressure system before use and could be stored for at least two months without a significant loss of vacuum force.

One-step self-powered automated sample loading

Once the chip had been sealed for at least twelve hours, the bag was cut open. The chip was removed and the aluminum foil covering the inlet was removed. In experiments, the LAMP

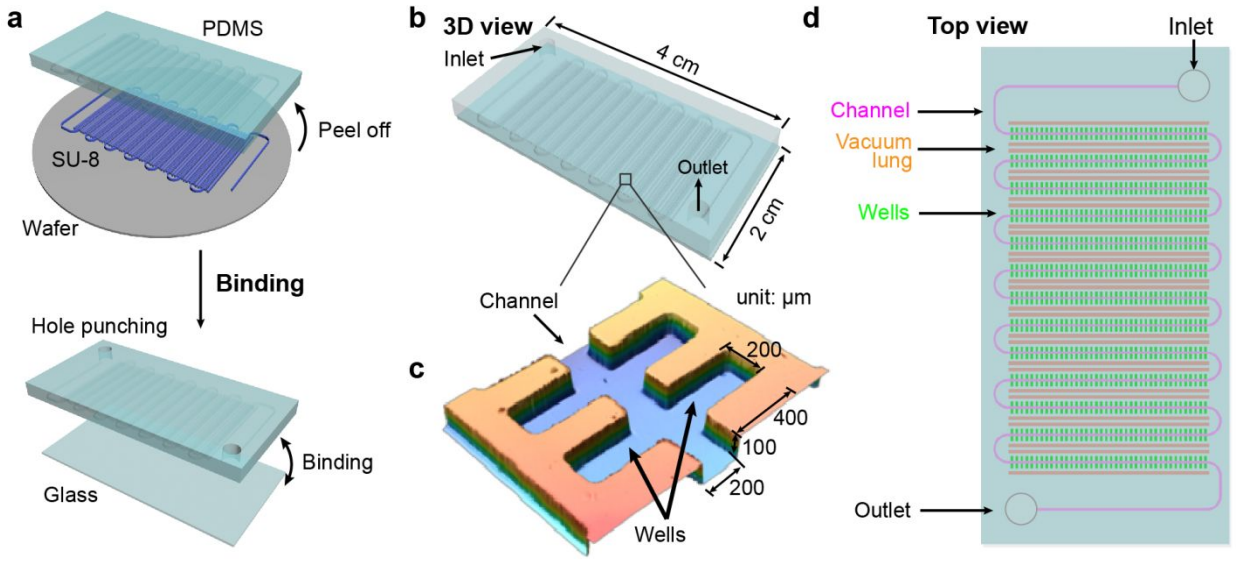

Fig. 1 The fabrication and characterization of SP-dChip. (a) Schematic illustration of the microfluidic chip fabrication process. PDMS is formed by using the SU-8 photoresist as the mould insert to create the microliter channels. After removing the PDMS from the wafer, inlet/outlet holes are punched, and the chip is bonded to a glass microscope slide. (b) Schematic design of the microfluidic chip with size dimensions. (c) 3D profilometry rendering of the fabricated microfluidic channels and wells with size dimensions (d) Top view of the microfluidic chip labelled with the channel, wells, inlet/outlet, and vacuum lungs.

solution (10 μL) was sucked in the pipette and the pipette tip was placed on the inlet. Due to the vacuum lung system, the fluid was passively self-driven through the channel into the wells. Afterwards, mineral oil (10 μL) was pipetted through to differentiate the wells. After four minutes, the foil over the outlet was removed to allow excess fluid to flow out of the chip. Once the sample digitization was complete, the inlet and outlet were wiped clean with a Kimwipe and disinfected with 70% ethanol. The inlet and outlets were then covered with an adhesive tape to secure samples in the system and avoid environmental contamination.

ZIKV RNA Isolation and Quantification

Viral RNA was isolated from infectious clones of Zika Virus.[34] Viral supernatants were treated with Benzonase (250 units/mL) diluted in 10× Benzonase Buffer[35, 36] and RNAse A (250 units/mL) to remove host nucleic acids.[37] Samples were then incubated for 37°C for three hours. RNA was extracted from the samples using the Zymo Quick-RNA Viral Kit. After extraction, the samples were purified using a 0.8× bead selection to removed small RNA fragments. The RNA was then quantified using RT-qPCR.

Reverse transcription loop-mediated isothermal amplification (RT-LAMP)

The RT-LAMP reaction was carried out by using the NEB WarmStart Fluorescent LAMP Kit following the standard protocol. Briefly, a 10× primer stock was created with 6 LAMP primers (16 μM FIP, 16 μM BIP, 4 μM LF, 4 μM LB, 2 μM F3, and 2 μM B3). The reaction mixture (25 μL) used for LAMP analysis consisted of LAMP 2× master mix (12.5 μL), LAMP primer mix (2.5 μL), target RNA (1 μL), and 5× LAMP fluorescent dye (0.5 μL). The reaction was incubated at 65°C for 30 min. The fluorescent signal was measured over time using a real-time PCR machine and subsequently characterized with gel electrophoresis.

Digital LAMP (dLAMP) to detect Zika Virus

Firstly, a stock solution of 20× calcein/manganese chloride ($MnCl_2$) was created, consisting of 500 nM calcein and 10 mM $MnCl_2$. The RT-LAMP reaction mixture (20 μL) was then prepared by mixing LAMP 2× master mix (10 μL), 10× primer mix (2 μL), target RNA (2 μL), and 20× calcein/$MnCl_2$ mix (1 μL). This reaction mixture (10 μL) was then loaded into the chips. Samples were digitized using the one-step self-powered automated loading method and incubated at 65°C for 1 hour before analysis.

Data acquisition and analysis

The SP-dChips were imaged using a scanning fluorescent microscope at 40× objective magnification over the entire chip. Images were subsequently analyzed using ImageJ software by converting to 8-bit to evaluate fluorescent intensity. The ratio of positive wells was manually counted and analyzed using the "analyze particles" tool in ImageJ.

Results and Discussions

Design of dLAMP microfluidic chip

The overview of the digital chip is shown in **Fig. 1**. The chip was manufactured and replicated using a photolithography process by using SU-8 as the mold insert on a silicon wafer, followed by punching inlet and outlet holes and bonding to a glass microscope (**Fig. 1a**).[28] The PDMS chip itself was designed to be 4 × 2 × 0.2 cm^3 (length × width × depth), as depicted by the 3D Studio Max rendering (**Fig. 1b**). The fabricated pattern dimensions on the PDMS were characterized using a 3D optical

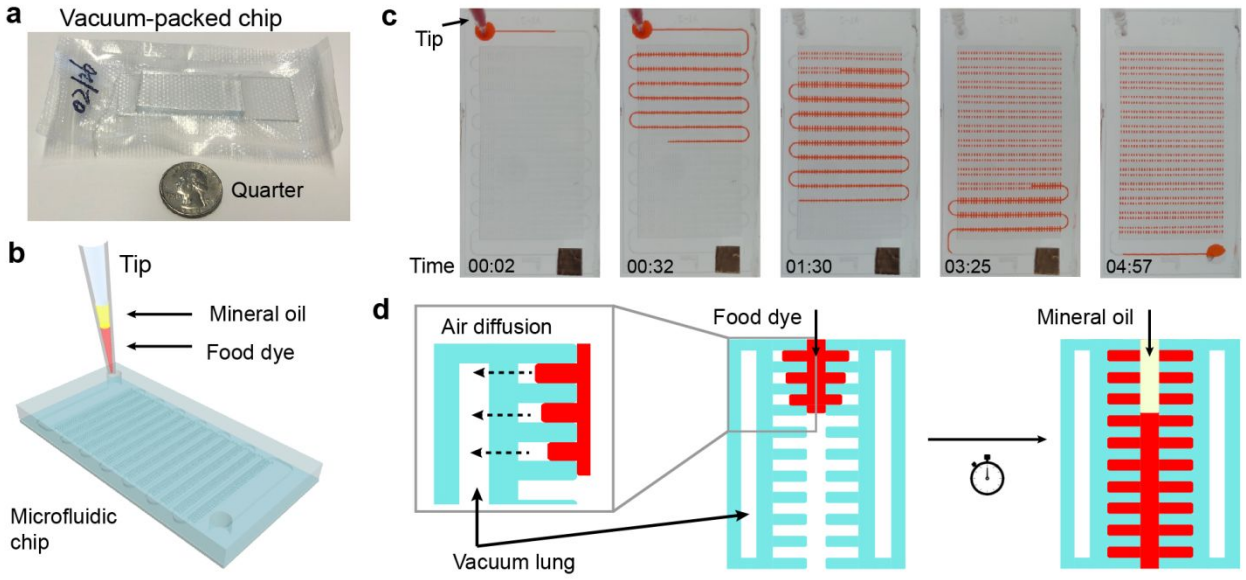

Fig. 2 Principle of the one-step automated sample loading system. (a) Photograph of the SP-dChip packaged in a vacuum bag with a U.S. quarter for size comparison. (b) Schematic illustration of the one-step automated loading method. (c) Chronological images displaying rapid sample digitization using food dye. (d) Schematic illustration of the vacuum lung system for well differentiation.

profilometry. In the design, the 200 µm wide channel leads to an estimated 400 x 200 x 100 µm nanoliter wells (**Fig. 1c**). A profilometric analysis of the manufactured chips shows that the real dimensions of the wells are around 125 µm wide and 88 µm deep once constructed, for an average volume of 7.04 nL (**Fig. S2**). The chip contains 1040 wells, each functioning as an individual reactor. In **Fig. 1d**, the channel, vacuum lungs, and wells are labeled in the top view with different colors. There are 24 rows of 40 wells with each row containing a vacuum lung directly behind the wells. As fluid flows through the channel, the vacuum lung system pulls the solution into the wells, allowing for sample digitization.

Principle of one-step automated sample loading

Prior to loading the sample solution, the microfluidic chip underwent degassing and was sealed within a vacuum bag (**Fig. 2a**). Due to the air permeability of the PDMS, the air within the cavities, including the channel, vacuum lungs, and wells, gradually permeated through the PDMS walls. This caused a reduction in air pressure in these cavities. Upon opening the vacuum bag, a pipette tip containing food dye at the base and mineral oil layered above the dye was promptly inserted into the inlet (**Fig. 2b**). Subsequently, as shown in **Fig. 2c** and **Movie S1**, the food dye passively flowed through the channel driven by

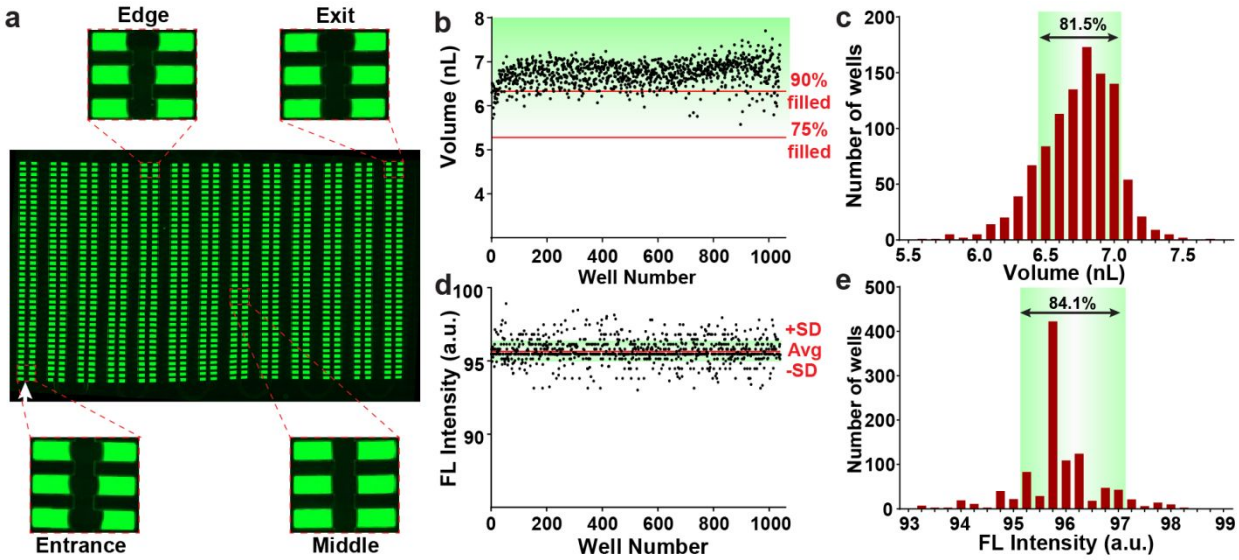

Fig. 3 Characterization of sample digitization and fluorescence in the SP-dChip. (a) Fluorescent image of the 1040 nanoliter wells filled with FITC fluorescent dye. (b) Volume of the microwells plotted from the entrance to the exit of the microfluidic chip. (c) Histogram of the nanoliter well volume distribution. (d) Fluorescent intensity of the 1040 wells plotted from the entrance to the exit. (e) Histogram of the fluorescent intensity values for the nanoliter wells.

the difference in air pressure between the wells and the vacuum lungs, eventually filling the wells completely. Upon priming the dye into the wells, mineral oil was dispensed to digitize each well as an independent reactor. Within 5 minutes, all 1040 wells were filled with food dye and effectively isolated by the mineral oil. The vacuum lungs, maintaining a low air pressure, facilitated the diffusion of air from the wells into the vacuum lungs, enabling the self-digitization of the food dye into the wells, as illustrated in **Fig. 2d**. The excess dye and mineral oil were removed through the outlet and the inlet and outlet ports were sealed using an adhesive tape. Our SP-dChip offers reduced operational complexity to enhance portability and user-friendliness when compared with other digital quantification methods, such as ddPCR, which rely on external pumping.

The uniformity of sample distribution and fluorescent intensity within the nanoliter wells

Ensuring uniform volumes within the wells is the key for maintaining experimental consistency and achieving optimal detection sensitivity. Upon packing the dLAMP chip in the vacuum-sealed bag, the energy required to propel the fluid flow becomes self-contained in the chip. Throughout the sample loading process, the solution quickly digitizes into the nanoliter wells until the oil-sealed compartmentalization is completed. To assess the uniformity of sample fluid distribution during the process, a solution containing fluorescein isothiocyanate (FITC) dye was introduced. After the digitization process, the chip was observed under the fluorescent microscopy at a 40× objective (**Fig. 3a**). The SP-dChip exhibited consistent volumes across its entirety, including the entrance, edges, middle, and exit of the channel. All areas displayed relatively uniform volumes and fluorescent intensity.

The fluorescent area and intensity of all 1040 wells were analyzed using ImageJ software. To determine the volume of fluid within each well, the fluorescent area was multiplied by a depth of 0.88 µm. Consequently, the average volumetric capacity of each well was estimated to be 7.04 nL and the average retained well volume was measured at 6.74 ± 0.27 nL, with a variance of 7.44% as depicted in **Fig. 3b**. All 1040 wells filled over 75% of the full volume, while 960 individual wells filled over 90% of the full volume. Additionally, 81.5% of the well volumes ranged between 6.5 and 7.1 nL, affirming the exceptional fluid flow and uniform distribution (**Fig. 3c**). The fluorescent intensity across wells also exhibited uniformity. Calculated from average fluorescent values across the middle of each nanoliter well, the mean fluorescent intensity was estimated as 95.58 a.u. ± 0.7621, with variations ranging from 93.20 to 99.11 a.u. (**Fig. 3d**). Impressively, 84.1% of the wells displayed fluorescent intensities between 95.1 and 97.1 (**Fig. 3e**), highlighting the excellent consistency for quantitative analysis.

LAMP detection of Zika Virus RNA

As a proof-of-concept demonstration, RT-LAMP-based quantitative detection of ZIKV was chosen owing to the high sensitivity and versatile capacity of LAMP for fluorescent analyses. Initially, we conducted bulk RT-LAMP reactions employing an intercalating fluorescent dye. In the amplification process, viral RNA undergoes reverse transcription into cDNA, subsequently forming dumbbell-loop DNA structures through the action of individual LAMP primers. The primer set operates cyclically to generate extensive DNA structures of varying lengths, which in turn bind to the intercalating dye, resulting in a robust fluorescent readout (**Fig. 4a**). Initially, four LAMP primer sets were optimized for the detection of ZIKV within 30 minutes. The primer set that displayed strong amplification of ZIKV RNA while avoiding primer dimerization or false positive amplifications was chosen for the assay (**Fig S3**). The LAMP

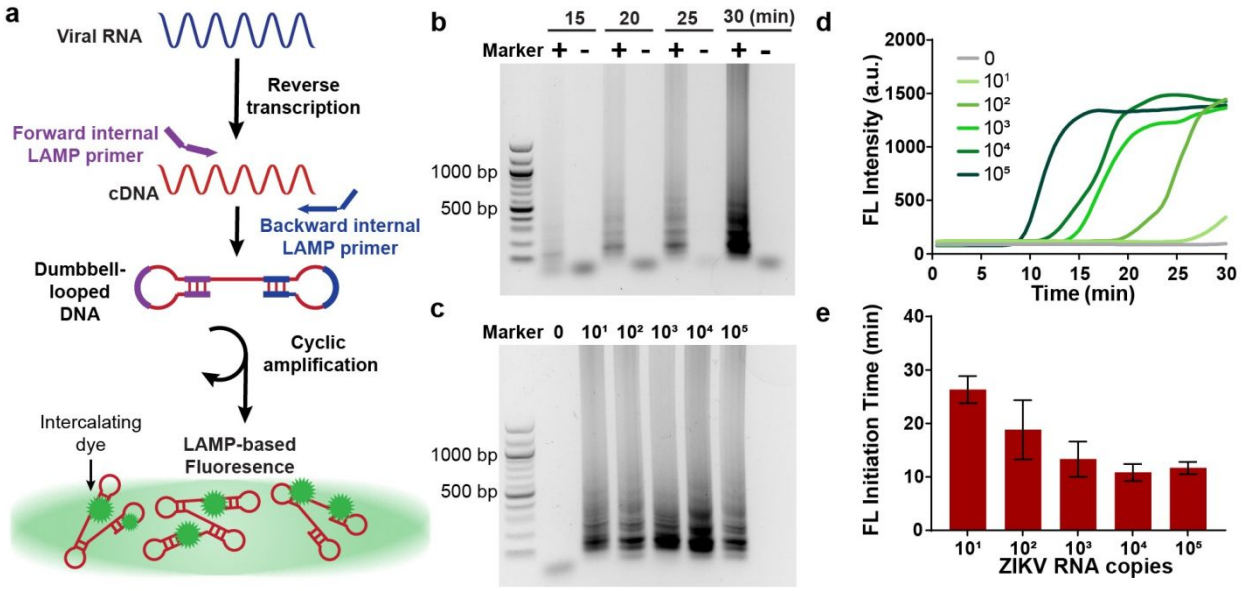

Fig. 4 LAMP detection of ZIKV RNA in a one-pot solution. (a) Schematic illustration of LAMP amplification and LAMP-based fluorescence using an intercalating dye. (b) Gel image of the negative control (-) and 10^4 ZIKV RNA copies (+) from 15 to 30 minutes. (c) Gel image of a range of 0 to 10^5 ZIKV RNA copies. (d) Fluorescent values over time of a range of 0 to 10^5 RNA copies. (e) Time to the initiation of a distinguishable fluorescent readout for 10^1 to 10^5 ZIKV RNA copies with three repeated trials.

primer set chosen for further analysis was initially developed in 2018 by Kaarj et al. In their experiments, the primers displayed high specificity for ZIKV when compared with Influenza A/H1N1.[38] In our experiments, we aimed to verify the primers sensitivity. As depicted in **Fig. 4b**, the amplification of 10^4 ZIKV RNA copies became visible within 15 minutes of incubation, steadily increasing over thirty minutes of heating. Notably, nonspecific amplification was absent within the 30-minute incubation period. Furthermore, a range of 10 to 10^5 ZIKV RNA copies underwent testing with a 30-minute incubation time (**Fig. 4c**). Amplification as low as 10 RNA copies was discernible after 30 minutes using gel electrophoresis.

We then evaluated the fluorescent signal over time utilizing a real-time quantitative PCR (RT-qPCR) system. In this process, the samples underwent reverse transcription followed by LAMP amplification. Samples containing 10^3 – 10^5 RNA copies exhibited a significant fluorescent signal within 15 minutes of incubation, reaching maximum fluorescence within 25 minutes (**Fig. 4d**). Lower amounts of RNA typically necessitated a longer time to initiate significant amplification for a discernible fluorescent signal. Further analysis of the time required for fluorescent initiation is shown in **Fig. 4e**. Fluorescent initiation was quantified as the time upon incubation at which the samples produced a distinguishable fluorescent signal in the RT-qPCR thermal cycler. For samples containing 10^3 or more ZIKV RNA copies, a fluorescent signal became apparent after approximately 11 minutes of heating. Conversely, samples containing lower copies often required an extended duration, with 10 ZIKV RNA copies taking up to 26 minutes to produce a distinct fluorescent signal. Collectively, these results underscore the efficacy of the RT-LAMP reaction for the ultrasensitive amplification of ZIKV RNA.

Digital LAMP Detection of ZIKV RNA

Following validation of the RT-LAMP reaction in bulk solutions, a quantitative model for the digital LAMP detection within the SP-dChip platform is developed. Unfortunately, the intercalating-dye approach for the fluorescent readout is not practical for simple microscopic imaging of digitized solutions. Instead, we utilized a calcein-based fluorescent method.[39] Calcein, a fluorescein metal indicator, along with manganese chloride ($MnCl_2$) is introduced to the LAMP reaction. The manganese ions (Mn^{2+}) serve to quench the calcein-based fluorescent signal. During the LAMP amplification, manganese ions form complexes with pyrophosphates from the amplification buffer, consequently releasing a fluorescent signal from the unquenched calcein.[40, 41] Magnesium ions (Mg^{2+}) from the solution bind to unbound calcein, which amplifies the fluorescent signal (**Fig. S4a**). Through experimentation with 25 nM calcein, we determined the optimal concentration of $MnCl_2$ to be 500 nM for a ratio of 20:1 $MnCl_2$ to calcein. (**Fig. S4b-c**).

Subsequently, the calcein-based RT-LAMP solution was evaluated for digital quantification of ZIKV RNA within the SP-dChip. Initially, we serially diluted the donated stock of ZIKV RNA containing 10^5 RNA copies/µL to concentrations ranging from 10^2 to 10^4 copies/µL. Repeated trials of each concentration involved incubating the digitized LAMP solution for one hour at 65°C, with subsequent analysis for amplification within the digitized nanoliter wells conducted via a fluorescent scanning microscope (**Fig. 5a**). Representative images displaying two rows of wells are presented in **Fig. 5b**. As the concentration rose from 10^2 to 10^4 copies/µL, the proportion of positive wells

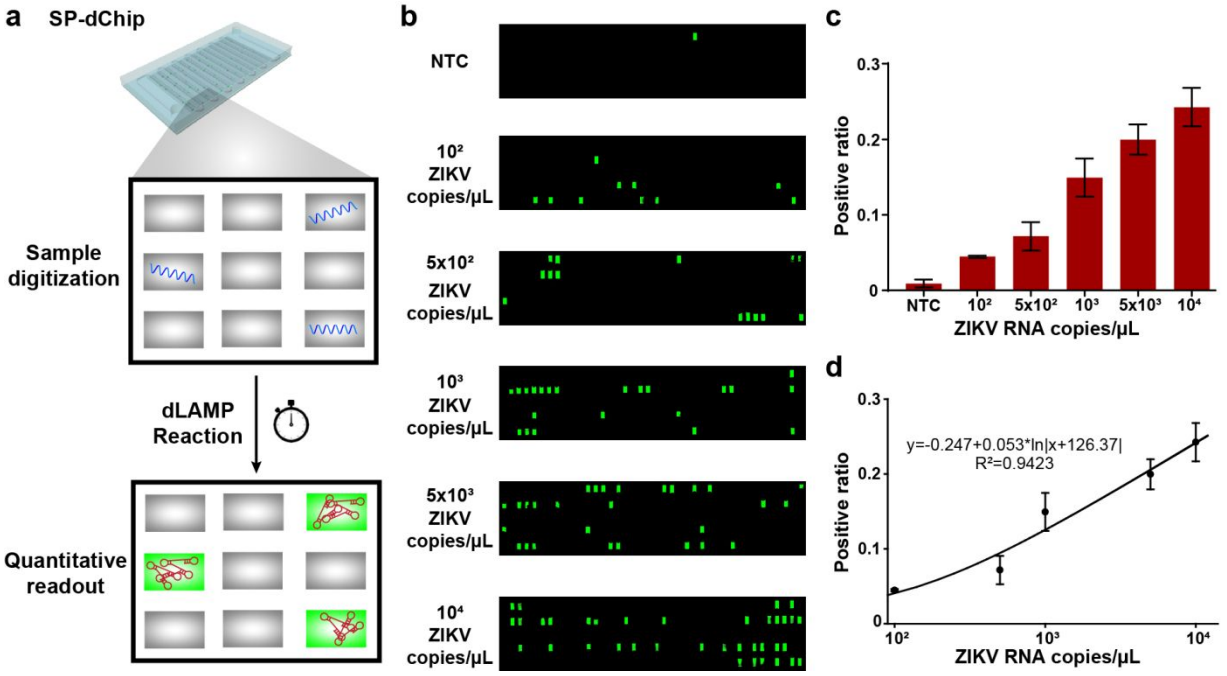

Fig. 5 Quantitative dLAMP detection of ZIKV RNA. (a) Schematic illustration of sample digitization and fluorescent quantitative detection within the SP-dChip. (b) Microscope images of two rows of the SP-dChip tested with a negative control and a range of 10^2 to 10^4 ZIK RNA copies/ µL. (c) Ratio of fluorescent wells for three repeated trials within the SP-dChip with a negative control and a range of 10^2 to 10^4 ZIK RNA copies/ µL. (d) Estimated ZIKV RNA copies per µL of solution fitted for the estimation of the ratio of positive fluorescent wells.

increased from an average of 4.47% to 24.26% (**Fig. 5c**). The negative control displayed sparse positive signals, with an average of 0.92% of the wells manifesting a fluorescent signal. The rate of false positive wells can be attributed to a number of potential factors including unusual isothermal multimerization and amplification,[42] uneven distribution of the fluorescent molecule or quenching agent, or minute contaminants. Notably, contamination is a common issue in LAMP-based amplification.[43] However, the digitization of samples into nanoliter wells before amplification mitigates the impact of challenging-to-eliminate contaminants, underscoring another advantage of our microfluidic system unoffered by bulk assays. Based on these findings, we devised a logarithmic model to forecast the estimated concentration of ZIKV RNA based on the observed percentage of fluorescent wells (**Fig. 5d**). The derived equation was determined to be $y = -0.247 + 0.053 * ln|x + 126.37|$, where x denotes the percentage of positive fluorescent wells for a sample exceeding 700 wells. Through this analysis, we concluded that our system could reliably estimate a range of 100 to 10^4 ZIKV RNA copies/µL, demonstrating sensitivity as low as 100 copies/µL. This level of sensitivity is optimal for the clinical detection of ZIKV.[44] These results affirm the efficacy of our SP-dChip in furnishing quantitative detection capabilities for emerging viruses through methodologies amendable to on-site applications.

Conclusions

In conclusion, the development of the SP-dChip represents a significant advancement in the field of POC diagnostics. By harnessing the principles of microfluidic design with a vacuum lung and vacuum packaging system, our SP-dChip offers the unique ability to provide completely passive sample digitization into individual nanoliter wells, facilitating high-throughput analysis while minimizing the risk of false positives and false negatives. We provide a robust and user-friendly platform for the rapid and quantitative detection of genetic materials. Unlike traditional POC devices, our system provides sensitive and reliable results without compromising portability with ease of use. Moreover, our chip's passive operation eliminates the need for external pumping or labor, making it ideal for on-site applications in resource-limited settings for the next generation of POC biosensors.

The SP-dChip could be an advanced tool for the detection of emerging viruses. By integrating a calcein-based fluorescent method, our SP-dChip demonstrates ultra-efficient sensitivity in quantifying the ZIKV RNA, with a detection limit as low as 100 copies/µL. The digitization of samples before amplification significantly reduces the impact of contamination in the LAMP reaction, thereby enhancing the accuracy of the platform. Through the development of a logarithmic model for estimating RNA concentrations based on fluorescent well counts, our system enables high precision and quantitative detection of ZIKV RNA. These results highlight the potential of our SP-dChip to revolutionize on-site diagnostics for the detection of emerging diseases, as the method could easily be extended to other emerging virus of interest. Therefore, we anticipate that our SP-dChip could contribute timely and effectively for the management of future infectious diseases on a global scale.

Challenges to our developed SP-dChip includes difficulty to mass-produce vacuum-sealed microfluidic chips, as mass production for PDMS chips is still underdeveloped in the industry. Additionally, as with any digital RT-LAMP devices, the largest hinderance for viral detection remains the difficulty of providing RNA extraction on-site. This manuscript provides a template for digital LAMP detection using a donated stock of ZIKV RNA. In the future, we aim to integrate microfluidic RNA extraction as well, which has been recently reported in microfluidic devices.

Author Contributions

We strongly encourage authors to include author contributions and recommend using CRediT for standardized contribution descriptions. Please refer to our general author guidelines for more information about authorship.

Conflicts of interest

There are no conflicts to declare.

Acknowledgments

This work was supported by the NIH National Institute of General Medical Sciences (R35GM147069) and the USDA National Institute of Food and Agriculture (2022-67021-36346)

Notes and references

1. P. B. Luppa, A. Bietenbeck, C. Beaudoin and A. Giannetti, *Biotechnology Advances*, 2016, **34**, 139-160.
2. A. Niemz, T. M. Ferguson and D. S. Boyle, *Trends in Biotechnology*, 2011, **29**, 240-250.
3. D. Liu, X. Li, J. Zhou, S. Liu, T. Tian, Y. Song, Z. Zhu, L. Zhou, T. Ji and C. Yang, *Biosensors and Bioelectronics*, 2017, **96**, 332-338.
4. Z. Qin, Z. Huang, P. Pan, Y. Pan, R. Zuo, Y. Sun and X. Liu, *Micromachines*, 2022, **13**, 2232.
5. K. Xu, R. Zhou, K. Takei and M. Hong, *Advanced Science*, 2019, **6**, 1900925.
6. X. Fu, Z. Cheng, J. Yu, P. Choo, L. Chen and J. Choo, *Biosensors and Bioelectronics*, 2016, **78**, 530-537.
7. S. Choudhary and Z. Altintas, *Biosensors*, 2023, **13**, 229.
8. Y. He, F. Jia, Y. Sun, W. Fang, Y. Li, J. Chen and Y. Fu, *Sensors and Actuators B: Chemical*, 2022, **369**, 132301.
9. N. Nesakumar, M. Lakshmanakumar, S. Srinivasan, A. Jayalatha Jbb and J. B. Balaguru Rayappan, *ChemistrySelect*, 2021, **6**, 10063-10091.
10. G. A. Posthuma-Trumpie, J. Korf and A. Van Amerongen, *Analytical and Bioanalytical Chemistry*, 2009, **393**, 569-582.
11. B. Vogelstein and K. W. Kinzler, *Proceedings of the National Academy of Sciences*, 1999, **96**, 9236-9241.

12. M. J. Jebrail and A. R. Wheeler, *Current Opinion in Chemical Biology*, 2010, **14**, 574-581.
13. O. Kalinina, J. Lebedeva I Fau - Brown, J. Brown J Fau - Silver and J. Silver.
14. A. R. Wheeler, *Science*, 2008, **322**, 539-540.
15. H. A. Biebuyck and G. M. Whitesides, *Langmuir*, 1994, **10**, 2790-2793.
16. S. M. Imani, R. Maclachlan, Y. Chan, A. Shakeri, L. Soleymani and T. F. Didar, *Small*, 2020, **16**, 2004886.
17. E.-C. Yeh, C.-C. Fu, L. Hu, R. Thakur, J. Feng and L. P. Lee, *Science advances*, 2017, **3**, e1501645.
18. G. M. Whitesides, *Nature*, 2006, **442**, 368-373.
19. S. P. Raju and X. Chu, *Journal of Medical Systems*, 2018, **42**.
20. J. Chen, Y. Zhou, D. Wang, F. He, V. M. Rotello, K. R. Carter, J. J. Watkins and S. R. Nugen, *Lab Chip*, 2015, **15**, 3086-3094.
21. C. Yi, C.-W. Li, S. Ji and M. Yang, *Analytica Chimica Acta*, 2006, **560**, 1-23.
22. M. E. Vincent, W. Liu, E. B. Haney and R. F. Ismagilov, *Chemical Society Reviews*, 2010, **39**, 974-984.
23. Y. Bai, E. Weibull, H. N. Joensson and H. Andersson-Svahn, *Sensors and Actuators B: Chemical*, 2014, **194**, 249-254.
24. K. F. Tjhung, S. Burnham, H. Anany, M. W. Griffiths and R. Derda, *Analytical chemistry*, 2014, **86**, 5642-5648.
25. J. J. Agresti, E. Antipov, A. R. Abate, K. Ahn, A. C. Rowat, J.-C. Baret, M. Marquez, A. M. Klibanov, A. D. Griffiths and D. A. Weitz, *Proceedings of the National Academy of Sciences*, 2010, **107**, 4004-4009.
26. C. Hu, W. Yue and M. Yang, *Analyst*, 2013, **138**, 6709-6720.
27. J.-C. Baret, *Lab Chip*, 2012, **12**, 422-433.
28. J. Chen, Y. Zhou, D. Wang, F. He, V. M. Rotello, K. R. Carter, J. J. Watkins and S. R. Nugen, *Lab on a Chip*, 2015, **15**, 3086-3094.
29. T. Xie, P. Wang, L. Wu, B. Sun, Q. Zhao and G. Li, *Lab on a Chip*, 2021, **21**, 3429-3437.
30. S. Yan, S. H. Tan, Y. Li, S. Tang, A. J. T. Teo, J. Zhang, Q. Zhao, D. Yuan, R. Sluyter, N. T. Nguyen and W. Li, *Microfluidics and Nanofluidics*, 2018, **22**.
31. V. Narayanamurthy, Z. E. Jeroish, K. S. Bhuvaneshwari, P. Bayat, R. Premkumar, F. Samsuri and M. M. Yusoff, *RSC Advances*, 2020, **10**, 11652-11680.
32. H. Lv, Z. Yang, J. Zhang, G. Qian, X. Duan, Z. Shu and X. Zhou, *Micromachines*, 2021, **12**, 883.
33. W. Lee, P. Tseng and D. Carlo, *Microtechnology for Cell Manipulation and Sorting*, 2017.
34. J. M. Marano and J. Weger-Lucarelli, *Frontiers in Cellular and Infection Microbiology*, 2023, **13**.
35. M. A. Rodgers, E. Wilkinson, A. Vallari, C. McArthur, L. Sthreshley, C. A. Brennan, G. Cloherty and T. De Oliveira, *Journal of Virology*, 2017, **91**, JVI.01841-01816.
36. J. Depew, B. Zhou, J. M. McCorrison, D. E. Wentworth, J. Purushe, G. Koroleva and D. E. Fouts, *Virology Journal*, 2013, **10**, 181.
37. A. Aryani and B. Denecke, *BMC Research Notes*, 2015, **8**.
38. K. Kaarj, P. Akarapipad and J.-Y. Yoon, *Scientific Reports*, 2018, **8**.
39. N. Tomita, Y. Mori, H. Kanda and T. Notomi, *Nature Protocols*, 2008, **3**, 877-882.
40. Y. Yao, N. Zhao, W. Jing, Q. Liu, H. Lu, W. Zhao, W. Zhao, Z. Yuan, H. Xia and G. Sui, *Sensors and Actuators B: Chemical*, 2021, **333**, 129521.
41. X. Jiang, W. Jing, X. Sun, Q. Liu, C. Yang, S. Liu, K. Qin and G. Sui, *ACS Sensors*, 2016, **1**, 958-962.
42. G. Wang, X. Ding, J. Hu, W. Wu, J. Sun and Y. Mu, *Scientific Reports*, 2017, **7**.
43. T. Waterfield, D. Fairley, B. Blackwood, J. McKenna and M. D. Shields, *BMC Pediatrics*, 2019, **19**.
44. S. J. R. D. Silva, K. Pardee and L. Pena, *Viruses*, 2019, **12**, 19.